Light Intensity Models for Annular UV Disinfection Reactors

The finite-length lamp model was compared to the infinite-length lamp model (or parallel radiation model) for annular reactors, specifically for the purpose of calculating average light intensities. Based upon the specified conditions that both models must apply equal energy to a reactor, such as is expected when the average surface flux of energy is measured by a chemical actinometric method, the results for the average intensity were very similar for the two models. Long lamp length and short reactor radius favored conditions where the finite-length model predicted a slightly higher average intensity than that calculated using the infinite-length model.

The inactivation of f2 virus was predicted in a completely mixed flow-through reactor using kinetic data obtained from batch reactions. For the particular flow-through reactor used, very little difference for the average intensity was calculated using the two intensity models. Indeed, predictions of reaction results using both models yielded results well within the range of experimental error.

M. T. Suidan
Department of Civil Engineering
University of Illinois
Urbana, IL 61801

B. F. Severin
Tennessee Eastman Company
Kingsport, TN 37662

Introduction

In modeling the efficiency of UV disinfection reactors, the average light intensity within the reactors is an important design and operating parameter. For single-lamp reactors of annular design, the average light intensity is encountered in the equations that describe inactivation in completely mixed, flow-through reactors and in perfect plug-flow reactors.

Two light intensity models, a radial approximation of the infinite line source model and the finite line source model, are compared based upon conditions of equal energy inputs. The problems addressed for each model are:

1. How to relate the total energy input to the reactor, such as measured with a chemical actinometer method, to the strength of a hypothetical line source of energy at the center of the UV lamp.

2. How to calculate the average of the local intensities at all points within the reactor based on the strength of the hypothetical line source.

Differences between the finite and infinite line source models are considered and the design conditions where the mathematically simpler infinite-length lamp model can be used without incurring excessive errors are discussed.

Inactivation results for an organism which displays simple mixed second-order inactivation kinetics, f2 bacterial virus, are presented. Inactivations were performed in a batch tray-type reactor and in a completely mixed, flow-through annular UV reactor. Results show that for the flow-through reactor evaluated in this study, excellent predictions can be made for the efficiency of the reactor using kinetic parameters taken from batch data, regardless of which of the two light intensity models is used to describe the flow-through reactor.

Model Development

In UV reactors the lamp is protected from the reaction solution by housing the lamp within a quartz tube. To facilitate calculation of intensity profiles, the effects of the air gap between the lamp and quartz tube on light transmission are neglected. Conditions are further simplified by assuming that the reflection or refraction of light at all interfaces is negligible. Figure 1 is a schematic drawing of a typical, annular UV reactor. Distance in the radial direction is represented by r where r_o is the outer radius of the quartz tube and $\bar{r}$ is the inner radius of the reactor wall. Light is assumed to be emitted from a hypothetical line source located at the center of the lamp. The variable z represents the vertical distance along the line source, and L is the total length of the line source. In the finite line source model, it is also necessary to define vertical distance within the reactor. This is given by the variable z_1, which varies from 0 to L. The line

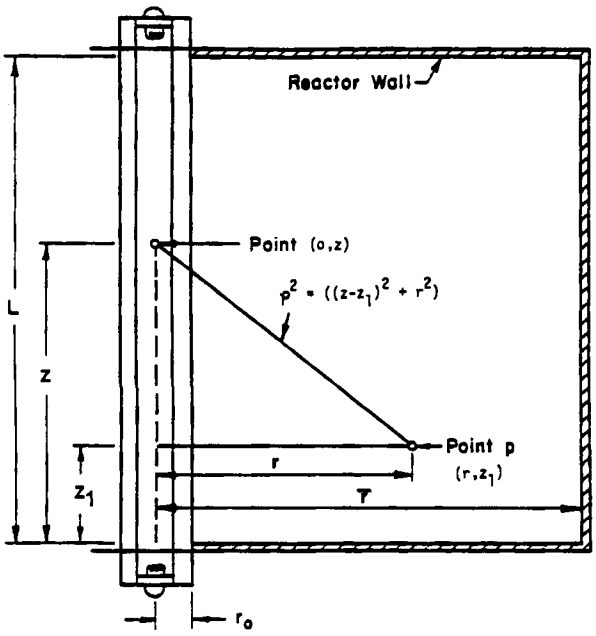

Figure 1. Geometric nomenclature for an annular UV reactor.

source emits a total of $I_\ell L$ of energy where I_ℓ is the strength of the line source. The quantity I_o is defined as the average flux of light energy, i.e., the total energy emitted per unit time per unit area averaged for the total surface of the quartz tube.

Radial approximation of the infinite line source model

In the infinite line source model all light is presumed to be emitted radially from the line source; i.e., the problem is one-dimensional and the energy flux varies as $1/r$. Due to axial symmetry it is recognized that the flux I_o is uniform everywhere at the quartz surface. Thus, if no light is absorbed between the line source and the quartz tube, energy emitted to the reactor is given by

$$I_\ell L = 2\pi r_o L I_o \tag{1}$$

The comparison of the infinite- and finite-length lamp models is based on equal energy inputs to the reactor. Equation 1 is presented as the definition of the input energy to a reactor from a radially emitting line source.

The light intensity, I, at any point p in the reactor is related to the surface flux, I_o, by a one-dimensional form of Lambert's law of absorption (Jacob and Dranoff, 1966)

$$\frac{1}{r}\frac{d(rI)}{dr} = -EI \tag{2}$$

where E is the monochromatic absorbance of water using logarithms to the base e. Integration of Eq. 2 using the limit $I = I_o$ when $r = r_o$ gives

$$I = I_o \frac{r_o}{r} e^{-E(r-r_o)} \tag{3}$$

Therefore, the average point intensity, $\bar{I}$, within an annular reactor is

$$\bar{I} = \frac{2I_o r_o}{(\bar{r}^2 - r_o^2)} \int_{r_o}^{\bar{r}} e^{-E(r-r_o)} dr \tag{4}$$

The integrated result is

$$m = \bar{I}/I_o = \frac{2r_o}{E(\bar{r}^2 - r_o^2)} [1 - e^{-E(\bar{r}-r_o)}] \tag{5}$$

where m is defined as the intensity factor and represents the ratio of the average point intensity in the reactor to the surface flux at the quartz tube. Equation 5 can be rewritten using dimensionless parameters $\alpha = Ar_o$ and $\epsilon = \bar{r}/r_o$

$$m = \frac{0.8686}{\alpha(\epsilon^2 - 1)} [1 - e^{-2.303\alpha(\epsilon-1)}] \tag{6}$$

where A is the absorbance coefficient using logarithms to the base 10 and $A = E/2.303$.

Finite line source

The finite line source model is based upon the premise that a lamp may be approximated by a series of point sources located along a line segment, and that light is emitted spherically from all points on the lamp axis. A differential element on the line source of length L and line intensity I_ℓ emits a point intensity of $I_\ell dz$. Within the reactor, each point p is subjected to light from all points on the line, and the intensity at p is given as the sum of the contributions from all of these points. The geometry of the finite line source is shown in Figure 1. The distance between a point in the reactor and a point on the line source is given as ρ where

$$\rho^2 = (z - z_1)^2 + r^2 \tag{7}$$

The dissipation of light from a point on the line source is given by Lambert's law of absorption (Jacob and Dranoff, 1970)

$$\frac{1}{\rho^2}\frac{d(\rho^2 I)}{d\rho} = -EI \tag{8}$$

which integrates to

$$I = \frac{I_\ell dz e^{-E[(z-z_1)^2+r^2]^{1/2}}}{4\pi[(z - z_1)^2 + r^2]} = \frac{I_\ell dz}{4\pi\rho^2} e^{-E\rho} \tag{9}$$

Equation 9 is further modified to account for no absorbance of light between a point on the line source and the quartz tube (Jacob and Dranoff, 1970)

$$I = \frac{I_\ell dz}{4\pi\rho^2} e^{-E\rho(r-r_o)/r} \tag{10}$$

Equation 11 is the special case where no absorbance occurs within the reactor

$$I = \frac{I_\ell dz}{4\pi p^2} \tag{11}$$

Consider the problem where I_ℓ is not known, such as the case where the energy input to the reactor is absorbed very near the lamp surface by a chemical reagent such as potassium ferrioxalate. If the light were emitted radially, no light would be lost out the top or the bottom of the quartz tube. However, if light is emitted in all directions, as in the case of a finite line source, then energy is lost from the top and bottom of the quartz tube. Therefore, I_ρ for the finite line model must be greater than I_ℓ for the infinite line model to obtain the same input energy into a reactor. The value of I_ℓ for the infinite line model is related to the average surface flux, I_o, by Eq. 12. The value of I_ℓ for the finite line model, however, is related to the average surface flux, I_o, by

$$I_\ell = 2\pi r_o I_o/\beta \tag{12}$$

where β is a transmission factor relating the ratio of energy transmitted to the reactor to the total energy emitted by the finite line source.

The transmission factor may also be calculated by considering the energy transmitted through the side of the quartz tube. Let z be the variable representing vertical distance on the line source and let z_1 represent the vertical distance along the outside of the quartz tube. The total energy transmitted through any level z_1 of the quartz tube is

Energy transmitted through (r_o, z_1)

$$= \int_{z=0}^{L} \frac{I_\ell r_o^2 dz dz_1}{2[(z - z_1)^2 + r_o^2]^{3/2}} \tag{13}$$

where a factor $r_o/[(z - z_1)^2 + r_o^2]^{1/2}$ has been introduced to correct for the angle of transmission of light through the quartz tube. Equation 13 is solved to give

Energy transmitted through (r_o, z_1)

$$= \frac{I_\ell dz_1}{2}\left[\frac{z_1}{\sqrt{z_1^2 + r_0^2}} - \frac{z_1 - L}{\sqrt{(z_1 - L)^2 + r_0^2}}\right] \tag{14}$$

The total energy transmitted through the quartz tube is

Energy transmitted =

$$\frac{I_\ell}{2}\int_o^L \left[\frac{z_1}{\sqrt{z_1^2 + r_0^2}} - \frac{z_1 - L}{\sqrt{(z_1 - L)^2 + r_0^2}}\right] dz_1 \tag{15}$$

The solution of Eq. 15 is

$$\text{Energy transmitted} = I_\ell\left(\sqrt{L^2 + r_o^2} - r_o\right) \tag{16}$$

and the fraction of energy transmitted is

$$\text{Fraction transmitted} = \beta = \sqrt{1 + (1/\ell)^2} - 1/\ell \tag{17}$$

where ℓ is the ratio of the lamp length to the radius of the quartz tube, $\ell = L/r_o$. Figure 2 shows how β varies with ℓ. For ℓ greater than 20, more than 95% of the energy from a finite line source enters the reactor. For ℓ greater than 100, more than 98% of the energy enters the reactor.

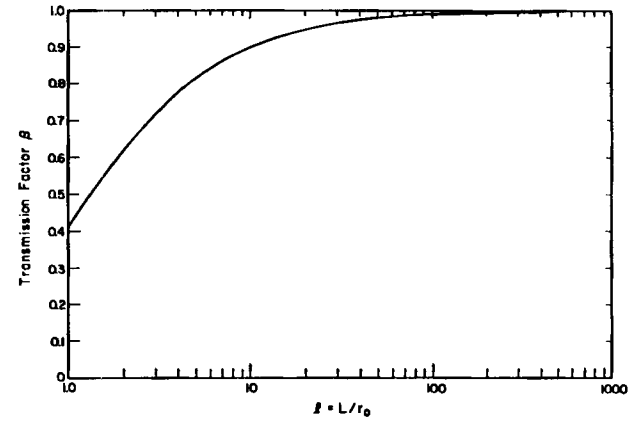

Figure 2. Fraction of energy transmitted into a reactor from a finite line source as a function of lamp geometry.

Another interesting feature of the finite-length lamp model is the relation of the surface flux at any height z_1 on the quartz tube, $I_f(r_o, z_1)$, to the average surface flux, I_o. The energy transmitted through (r_o, z_1) from a finite-length lamp is given by Eq. 14. Therefore, the flux per unit area of the cylindrical surface at z_1 is

$$I_{f(r_o,z_1)} = \frac{I_\ell}{4\pi r_o} \cdot \left\{\frac{(z_1/L)}{\sqrt{(z_1/L)^2 + (1/\ell)^2}} - \frac{(z_1/L) - 1}{\sqrt{[(z_1/L) - 1]^2 + (1/\ell)^2}}\right\} \tag{18}$$

To relate this to the average surface flux, I_o, the term I_ℓ in Eq. 18 may be substituted with its definition in accordance with a finite line source, Eq. 12. Therefore, the ratio of $I_f(r_o, z_1)$ to I_o is

$$\frac{I_{f(r_o,z_1)}}{I_o} = \frac{1}{2\beta} \cdot \left\{\frac{(z_1/L)}{\sqrt{(z_1/L)^2 + (1/\ell)^2}} - \frac{(z_1/L) - 1}{\sqrt{[(z_1/L) - 1]^2 + (1/\ell)^2}}\right\} \tag{19}$$

Since I_o is also the average flux emitted by an infinite-length lamp, Eq. 19 also serves to compare the flux calculated using the two models at any height z_1 on the quartz tube.

Figure 3 shows the ratio of the surface flux to the average flux $(I_{f(r_o,z_1)}/I_o)$, relative to the distance along the lamp surface, z_1/L, for a variety of lamp dimensions, $\ell = L/r_o$. The lower the value of ℓ, the more concentrated the flux is toward the center of the lamp. For lamps with large ℓ, the distribution of flux along the lamp surface is more uniform.

With this background, it is now possible to continue the development of the equations for the light intensity profiles within the reactor using the finite-length lamp model. Consider the case where no absorbance of light occurs within the reactor. From Eq. 11 the average point intensity at a constant radius $\bar{I}_r$ is given by

$$\bar{I}_r = \frac{1}{L}\int_o^L \int_o^L \frac{I_\ell dz dz_1}{4\pi[(z - z_1)^{2+}(r^2)]} \tag{20}$$

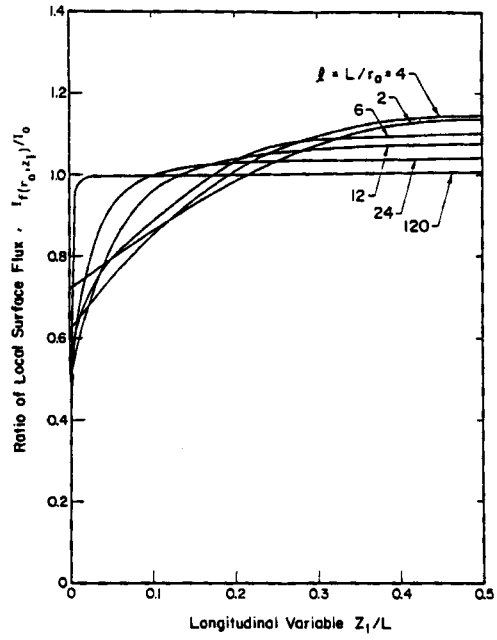

Figure 3. Distribution of energy flux from a finite line source along a cylindrical surface.

Equation 20 is solved to give

$$\bar{I}_r = \frac{I_\ell}{2\pi r L}\left\{L\tan^{-1}\left(\frac{L}{r}\right) - \frac{r}{2}\ln\left[1 + (L/r)^2\right]\right\} \qquad (20)$$

It is cautioned here not to confuse $\bar{I}_{r_o}$, the average point intensity calculated at $r = r_o$, with an average value of $I_{f(r_o,z_1)}$, the flux at the surface of the quartz tube.

The average point intensity in the reactor for the case of no absorbance is given by Eq. 21.

$$\bar{I} = \frac{I_\ell}{\pi L(\bar{r}^2 - r_o^2)}\int_{r_o}^{\bar{r}} \cdot\left\{\left[L\tan^{-1}(L/r) - \frac{r}{2}\ln\left(1 + (L/r)^2\right)\right]\right\} dr \qquad (22)$$

which is integrated to give

$$\bar{I} = \frac{I_\ell \ell}{r_o\pi(\nu^2 - 1)}\left\{\frac{\nu}{\ell}\tan^{-1}(\ell/\nu) - \frac{1}{\ell}\tan^{-1}(\ell) + \frac{1}{4}\ln\frac{\ell^2 + \nu^2}{\ell^2 + 1} - \frac{1}{4}\left[\left(\frac{\nu}{\ell}\right)^2\ln\frac{\ell^2 + \nu^2}{\nu^2} + \frac{1}{4\ell^2}\ln(\ell^2 + 1)\right]\right\} \qquad (23)$$

This is related to the average surface flux, I_o, by Eq. 12

$$\bar{I}/I_o = \chi = \frac{2\ell}{\beta(\nu^2 - 1)}\left[\frac{\nu}{\ell}\tan^{-1}(\ell/\nu) - \frac{1}{\ell}\tan^{-1}(\ell) + \frac{1}{4}\ln\frac{\ell^2 + \nu^2}{\ell^2 + 1} - \frac{1}{4}\left(\frac{\nu}{\ell}\right)^2\ln\frac{\ell^2 + \nu^2}{\nu^2} + \frac{1}{4\ell^2}\ln(\ell^2 + 1)\right] \qquad (24)$$

The dimensionless parameter, χ, is introduced as the ratio of the average point intensity in the reactor to the average flux at the surface of the quartz tube.

Some interesting relations can be developed by comparing the two intensity factors m and χ in waters with no absorbance. Under the conditions where the absorbance is zero, m simplifies to

$$m = 2/(\nu + 1) \qquad (25)$$

It is important to note that while m is dependent only on ν, χ is dependent on both ν and ℓ. The interesting aspect of this comparison is that with certain reactor designs, the finite-length lamp model predicts higher average point intensities than does the infinite-length lamp model. Lower values of ν and higher values of ℓ favor conditions where χ is greater than m.

To help visualize why this occurs, one special case, where m is exactly equal to χ, was analyzed. As an example, when ν is 6, m equals χ when ℓ is 11.159. Figure 4 was developed using these values of ν and ℓ. Light intensity profiles at various values of r/r_o, the dimensionless variable in the radial direction, up to $r/r_o = \nu = 6$ for selected relative vertical distances, z_1/r_o, are shown. The solid line represents point intensities calculated using the infinite-length lamp model relative to the average flux at the surface of the quartz tube. The broken lines represent point intensities calculated using the finite-length lamp model relative to the average surface flux. However, since the average surface flux is exactly equal to the surface point intensities from an infinite-length lamp, this figure can also be interpreted as the comparison of the point intensities generated by the two models. The point intensities for the finite-length lamp model were developed from the expression for no UV absorbance within the reactor

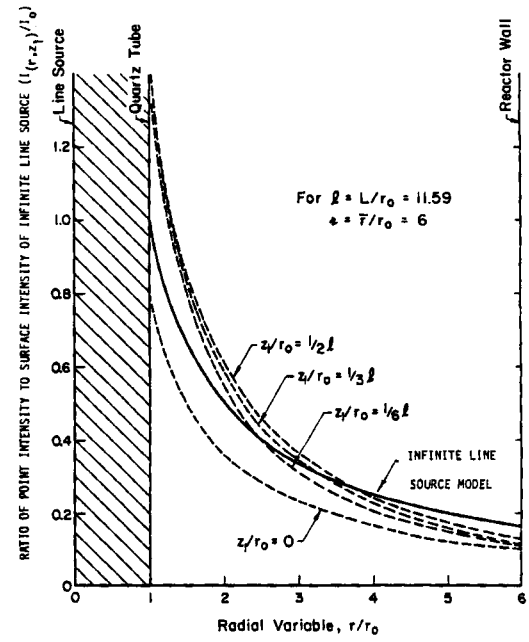

Figure 4. Comparison of calculated point intensities in an annular reactor.

— Infinite-length lamp model
---- Finite-length lamp model

where the point intensity at (r, z_1), $I_{(r,z_1)}$, is

$$I_{(r,z_1)} = \int_o^L \frac{I_\ell dz}{4\pi[(z - z_1)^2 + r^2]} \tag{26}$$

which is integrated to give

$$I_{(r,z_1)} = \frac{I_\ell}{4\pi r}\left\{\tan^{-1}\left(\frac{z_1/r_o}{r/r_o}\right) - \tan^{-1}\left[\frac{(z_1/r_o) - \ell}{r/r_o}\right]\right\} \tag{27}$$

Substitution for I_ℓ with Eq. 12 yields

$$I_{(r,z_1)} = \frac{I_o}{2\beta}\left(\frac{r_o}{r}\right)\left\{\tan^{-1}\left(\frac{z_1/r_o}{r/r_o}\right) - \tan^{-1}\left[\frac{(z_1/r_o) - \ell}{r/r_o}\right]\right\} \tag{28}$$

Figure 4 shows that the point intensity, as calculated using the finite-length lamp model, is always lower than that calculated using the infinite-length lamp model when $z_1/r = 0$. However, for z_1/r_o equal to $\ell/6$, $\ell/3$, or $\ell/2$, point intensities near the lamp, as calculated using the finite-length model, are higher than those calculated using the infinite-length model. As r/r_o approaches the radial distance $\epsilon = 6$, the point intensities calculated using the finite-length model are less than those calculated using the infinite-length lamp model. For the chose case, the overall average intensities are equal for the two models. However, if the distance to the reactor wall were slightly larger, then χ would be less than m, and if the distance to the reactor wall were decreased, then χ would be larger than m.

With UV-absorbing materials in the water, the average point intensity $\bar{I}$ for the finite-length lamp model can be written as

$$\bar{I} = \frac{I_\ell}{2\pi L(\bar{r}^2 - r_o^2)} \int_{r_o}^{\bar{r}} \int_o^L \int_o^L \cdot \frac{e^{-E[(z-z_1)^2 + r^2]^{1/2}(r - r_o)/r]} r dr dz dz_1}{[(z - z_1)^2 + r^2]} \tag{29}$$

With the substitution of I_ℓ using the definition of Eq. 12 and with conversion to dimensionless form, Eq. 29 may be rewritten

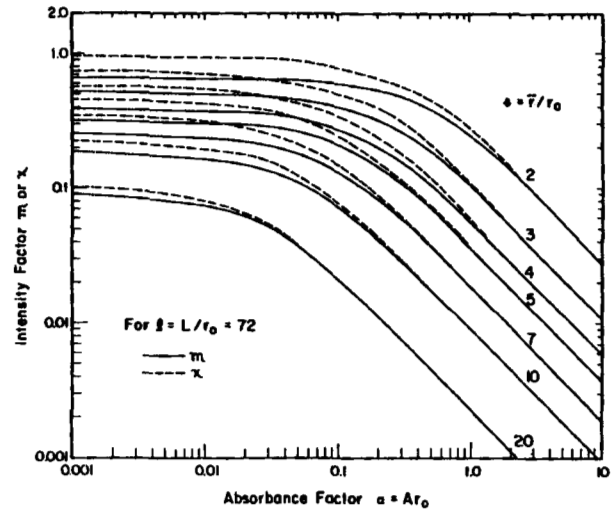

Figure 6. Intensity factors for an annular reactor with $\ell = L/r_o = 72$.

to give an expression for χ

$$\frac{\bar{I}}{I_o} = \chi = \frac{1}{\beta(\epsilon^2 - 1)} \int_1^{\epsilon} \int_1^{\ell} \int_0^{\ell} \cdot (e^{-2.303\alpha[[(z/r_o) - (z_1/r_o)]^2 + (r/r_o)^2]^{1/2}[1 - (r_o/r)]}) \cdot \left\{\frac{(r/r_o)d(r/r_o)d(z/r_o)d(z_1/r_o)}{[(z/r_o) - (z_1/r_o)]^2 + (r/r_o)^2}\right\} \tag{30}$$

An analytical solution for Eq. 30 was not found. Consequently, numerical solutions were obtained. The limits of Eq. 30 are known for the case of no absorbance (Eq. 24) and for the case of very high absorbance. By a conservation of energy, χ must be equal to m in waters with high UV absorbance.

Figures 5, 6, and 7 present χ as a function of $\alpha = Ar_o$. Each figure represents a different reactor dimension ℓ. Reactor dimensions of $\ell = 24$ (Figure 5), $\ell = 72$ (Figure 6), and $\ell = 120$ (Figure 7) were chosen because of the availability of UV lamps

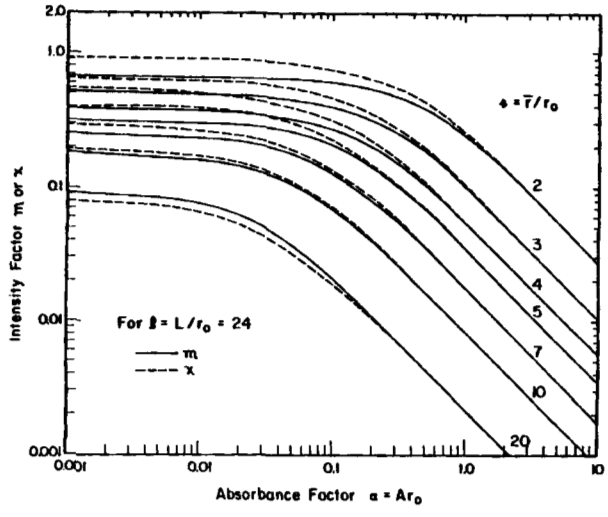

Figure 5. Intensity factors for an annular reactor with $\ell = L/r_o = 24$.

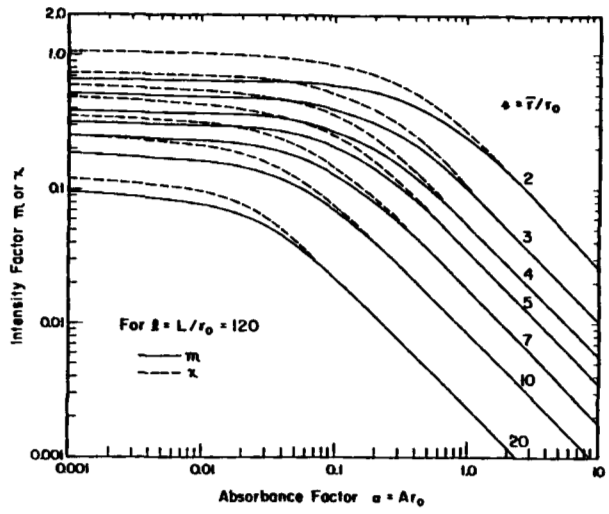

Figure 7. Intensity factors for an annular reactor with $\ell = L/r_o = 120$.

in lengths of 30.5, 91.4, and 152.4 cm. A typical radius for quartz tubes is 1.27 cm. Solutions for a range of ϵ from 2 to 20 are given in each figure. Solid lines represent solutions for m and are given as a reference. Since m is independent of ℓ, these lines are the same in each of the three figures. Broken lines represent solutions for χ. For most conditions of ℓ and ϵ presented in these figures, χ is larger than m for low values of α. The only case where χ is less than m is shown for $\ell = 24$ and $\epsilon = 20$, Figure 5. In all cases, as the absorbance of the water increases, as given by α, the value of χ tends to move toward m. This is consistent with a conservation of energy input in the two models. Some practical observations can be made from these figures. Lukiesh and Holladay (1944) reported a range of absorbances of $A = 0.016$ to 0.024 cm^{-1} for waters from three public water supplies. Severin (1980) indicated a range of $A = 0.07$ to 0.10 cm^{-1} for secondary treated wastewater effluents. Assuming $r_o = 1.27$ cm, expected values of α for typical UV disinfection reactor applications range from about 0.02 to 0.13. For this range it is seen that χ is very nearly equal to m. Therefore, for most practical applications, m is an adequate assessment of the average intensity within an annular UV reactor.

Mixed second-order kinetics

For organisms that express mixed second-order inactivation kinetics, the models for batch reactors and completely mixed, flow-through annular reactors are quite simplistic. The equation for inactivation in a batch reactor in which UV intensity can be considered everywhere uniform, is given by

$$\frac{N}{No} = e^{-k\bar{I}t} \tag{31}$$

where t is batch exposure time. For a completely mixed reactor of annular design, the mixed second-order rate expression becomes

$$\frac{N}{No} = \frac{1}{1 + mkI_o t} \tag{32}$$

when the infinite line source intensity model is used and,

$$\frac{N}{No} = \frac{1}{1 + \chi kI_o t} \tag{33}$$

when the finite line source model is used. The term t is introduced as the theoretical retention time in the flow-through reactor.

Experimental Equipment and Procedures

Continuous-flow disinfection data were developed using a completely mixed, single-lamp annular reactor made from a 14.0 cm ID Plexiglas column, 27 cm in height, as illustrated in Figure 8. The volume of the reactor, excluding the volume of the quartz tube, was 4,010 cm^3. A 2.54 cm OD quartz tube housed a General Electric Voltare UV-LUX g10T5 ½ low-pressure mercury vapor lamp, powered by a Universal Mfg. Co. (Patterson, NJ) Thermomatic-X fluorescent lamp DC ballast. Voltage (140 V) was supplied by a Variac voltage regulator (General Radio Company, Concord, MA). The inside wall of the reactor was painted with lampblack to minimize reflection. The incident

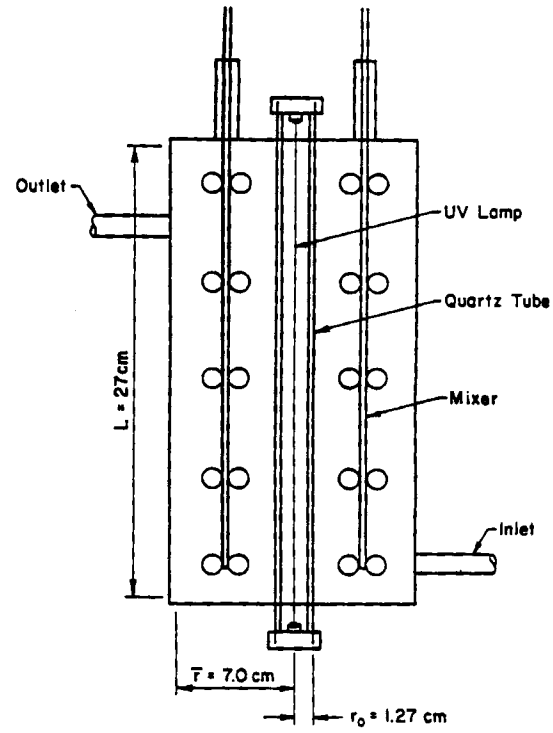

Figure 8. Completely mixed, flow-through UV reactor.

light intensity at the surface of the quartz tube (34,000 $\mu w/cm^2$) was measured using the potassium 2 ferrioxalate chemical actinometry test (Calvert and Pitts, 1966). Complete mixing in the reactor was achieved by the use of two impeller systems placed on opposite sides of the reactor. Each impeller shaft contained five equally spaced, three-bladed impellers. The shafts were driven by Fisher Scientific Co. Dyna-mix motors rated at 6,000 rpm and at about 85% of capacity. The reactor was operated under a slight head to eliminate free face vortexing. Flows could be adjusted to provide retention times between 20 and 260 s.

In terms of dimensionless quantities, the completely mixed flow-through reactor had an $\epsilon = 5.47$ and $\ell = 21.3$. For a reactor with these dimensions, χ is only slightly larger than m for values of α less than 0.1, and is essentially equal to m for values of α greater than 0.1. Because of the similarity of m and χ for this reactor, it was expected that either model would apply equally well. For convenience of comparison, Figure 9 gives χ and m for the annular reactor as a function of UV absorbance.

Water used in the experiments with the flow-through reactor was prepared in a 200 L reservoir by adding 1 L of stock phosphate buffer solution (24 g KH_2PO_4 and 6 g NAOH per L stock) and appropriate volumes of f2 virus stock and UV light-attenuating agent to 200 L deionized (DI) water. The buffer maintained the pH between 6.5 and 7.0; viral densities in the test water varied between 2×10^5 and 1×10^6 plaque-forming units (pfu) per mL. The UV-attenuating agent was parahydroxybenzoic acid (PHBA), which has a narrow absorbance peak around 244 nm. PHBA was used to simulate natural tannic acid components present in wastewater. Quantities up to 500 mL of a stock PHBA solution (10 g/L) added to 200 L DI water provided a range of absorbance A, (base 10) at 254 nm, between 0.04 and 2.2 cm^{-1}. The absorbance of the test water was measured on an ACTA III Spectrophotometer (Beckman, Ind., London, En-

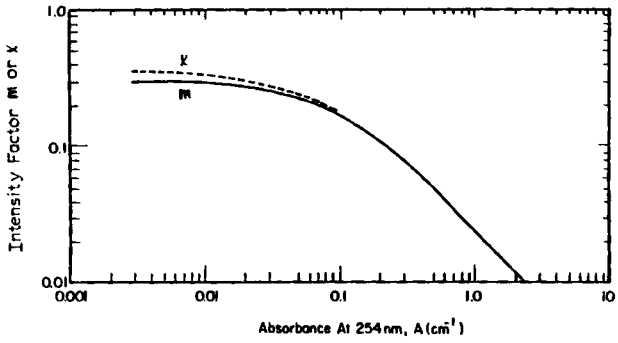

Figure 9. Intensity factors, m and χ, for the experimental flow-through annular reactor.

gland). PHBA in this range of concentrations was not toxic to the microorganisms. The temperature of the test water was 20 ± 1.0°C.

Batch disinfection data were generated using a flat-tray reactor with a 2.54 cm water depth and a total volume of 500 mL. The UV source was a General Electric G15T8 lamp mounted in a parabolic stainless steel reflector, and utilizing a Sylvania FS-2 Glostat ballast at line voltage. The lamp was placed 63 cm above the surface of the water. A shutter arrangement was used to control exposure time. A magnetic stirrer provided mixing in the reactor. The UV intensity at the surface of the water was measured to be 450 $\mu w/cm^2$ using the potassium ferrioxalate chemical actinometry test. Test water used in the batch reactor was prepared by adding 2.5 mL of stock phosphate buffer solution and 500 mL DI water to the reactor. This solution was then sterilized for 5 min with UV prior to the addition of organisms. The f2 virus densities ranged from 2×10^5 to 1×10^6 pfu per mL test water. The pH of the water was between 6.5 and 7.0, and the temperature of the water was 20 ± 1.0°C. No PHBA was added to the water, and in all tests the UV absorbance was below 0.04 cm^{-1}. At this level, the average intensity through the water column was approximately 95% of the input energy flux at the water surface.

Initial cultures of bacterial virus f2 and host organism, *E. coli* K-13 were obtained from Vincent Oliveri, The Johns Hopkins University, Baltimore, MD. Bacterial virus f2 was cultured and enumerated using modifications of the method described by Leob and Zinder (1961). Host cultures of *E. coli* K-13 were grown in TYE broth (tryptone 10 g/L, yeast extract 1 g/L, and sodium chloride 8 g/L) at 37°C on a shaking water bath. Stock virus suspensions were prepared by the addition of the virus (0.1 infectivity ratio of virus to bacteria) to pregrown cultures of *E. coli* K-13 at a density of approximately 3×10^8 bacteria/mL. After lysis of the infected culture for 8–12 h at 37°C on a shaking water bath, cell debris was removed by centrifugation at 2,500 rpm for 15 min (Sorval model GLC-2 lab centrifuge, type HL-4 rotor head, Sorval Inc., Newtown, CT). The supernatant liquor, containing the virus stock, was maintained in 5 mL aliquots at 4°C. Virus density was determined using an agar overlay method. TYE agar (10 g agar/L TYE broth) plates and fresh cultures of host bacteria were prepared in advance of each day of testing. Just prior to use, 1 mL of a sterile stock solution of calcium chloride (22 g/L) was added to each 20 mL of host bacteria culture. Three drops of the bacteria culture, to provide a lawn of host cells, and 0.1 mL of a proper dilution of virus suspension were then added to 3 mL of melted TYE agar. This mixture was then poured over a hardened agar plate. Plaques were counted after 8–24 h incubation at 35°C.

Results

Batch inactivation data from five independent experiments are presented in Figure 10. Each point represents the numerical average of triplicate enumerations. A least-squares regression analysis of the natural logarithm of the fraction survival vs. contact time, fitted to Equation 31, yielded a slope, $k\bar{I} = 0.03258$, with a regression coefficient (r^2) of 0.986. From knowledge of the value of $\bar{I}$, the value of $k = 0.072 \times 10^{-3}$ $cm^2/\mu w \cdot s$ was obtained.

Nine experiments were performed in the completely mixed, flow-through reactor. Absorbances of the test water were varied from 0.03 to 2.20 cm^{-1} by the addition of PHBA. Each experiment was performed at a constant absorbance while contact times were varied from approximately 20 to 260 s. The form of Eqs. 32 and 33 indicates that given good estimates of k, I_o, and m or χ, the entire set of nine experiments can be plotted on one curve of N/N_o vs. either mkI_ot or χkI_ot. Figure 11 gives the inactivation data as a function of mkI_ot, while an almost identical figure was obtained when the data were plotted as a function of χKI_ot. The solid line in Figure 11 represents the model prediction. Both models fit the data well within the range of scatter. Regression coefficients were calculated between observed results and model predictions. Using m, and r^2 value of 0.961 was obtained, while the use of χ resulted in an r^2 value of 0.956. The difference is not felt to be important.

While the differences in the two models is apparently less than the experimental error incurred in using a completely mixed, flow-through reactor, it must be pointed out that in plug flow the small differences in the model would naturally result in an increased difference in the data.

Conclusions

1. The finite-length lamp light model was compared to the infinite-length lamp model under the specified condition that

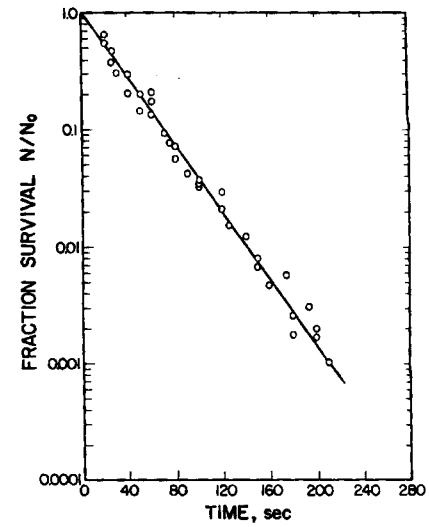

Figure 10. Batch inactivation data.
O Numerical average of triplicate enumerations

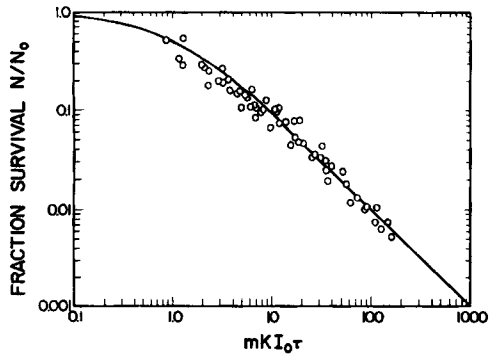

Figure 11. Prediction of flow-through reactor results using infinite-length lamp model.
— Model prediction

equal energy inputs are provided to an annular reactor. For situations where the average intensity within the reactor is adequate to define kinetic rates, there is no practical reason to use the more complex finite-length lamp model instead of the infinite-length lamp model. In many cases, especially for reactors with large length to lamp radius ratios and overall reactor radius to lamp radius ratios, the finite-length model can predict higher average intensities than can the infinite-length model.

2. The inactivation of bacterial virus f2 was determined in a batch reactor and in a completely mixed, flow-through reactor. A mixed second-order kinetic constant was obtained from the batch data. This constant, along with the average intensities calculated for the flow-through reactor using both intensity models, was used to predict the flow-through reactor results. Excellent predictions were obtained using both models. It had been judged that the simpler light intensity model would perform as well as the more complex model. Both models predicted results well within the scatter of the observed data.

Acknowledgment

The authors are grateful to Arthur Robinson, University of Illinois at Urbana-Champaign, for valuable insights into this project. This research was supported by the Department of Civil Engineering at the University of Illinois at Urbana-Champaign.

Notation

A = monochromatic absorbance of water using base 10 = $E/2.303$, cm^{-1}
E = monochromatic absorbance of water using natural logarithms, cm^{-1}
I = light intensity at any point p in reactor, $\mu w/cm^2$
I_f = surface flux of light energy at any height z_1 on quartz tube, $\mu w/cm^2$
I_ℓ = strength of line source, $\mu w/cm$
I_o = average flux of light energy at surface of quartz tube, $\mu w/cm^2$
$\bar{I}$ = average point light intensity within annular reactor, $\mu w/cm^2$
$\bar{I}_r$ = average point light intensity at a constant radius, $\mu w/cm^2$
k = mixed second-order inactivation rate constant, $cm^2/\mu w \cdot s$
L = total length of line source, cm
ℓ = ratio of lamp length to radius of quartz tube = L/r_o
m = intensity factor for infinite line source model = $\bar{I}/I_o$
N = density of viable microorganisms, cm^{-3}
N_o = initial or influent density of viable microorganisms, cm^{-3}
r = radial distance in annular reactor, cm
r_o = outer radius of quartz tube, cm
$\bar{r}$ = inner radius of reactor wall, cm
ν = ratio of reactor inner radius to quartz tube outer radius = $\bar{r}/r_o$
t = time, s
z = vertical distance along line source, cm
z_1 = vertical distance within annular reactor, cm

Greek letters

α = absorbance of water = Ar_o
β = transmission factor for finite line source
ρ = distance between a point in reactor and a point on finite line source, cm
μ = intensity factor for finite line source model = $\bar{I}/I_o$

Literature cited

Calvert, J. G., and J. N. Pitts, *Photochemistry*, Wiley, New York, 783 (1966).

Jacob, S. M., and J. S. Dranoff, "Radial Scale-up of Perfectly Mixed Photochemical Reactors," *Chem. Eng. Prog. Symp. Ser.*, **62**(68), 47 (1966).

——— "Light Intensity Profiles in a Perfectly Mixed Photoreactor," *AIChE J.*, **16**(3), 359 (1970).

Leob, T., and N. Zinder, "A Bacteriophage Containing RNA," *Proc. Nat. Acad. Sci. U.S.*, **47**, 282 (1961).

Luckiesh, M., and L. L. Holladay, "Disinfecting Water by Means of Chemical Lamps," *General Electric Rev.*, **47**(4), 14 (1944).

Severin, B. F., "Disinfection of Municipals Wastewater Effluents with Ultraviolet Light," *J. WPCF*, **52**, 2007 (1980).

Manuscript received Jan. 14, 1986, and revision received April 9, 1986.